Journal of Chemical Neuroanatomy 68 (2015) 1–13

Contents lists available at ScienceDirect

Journal of Chemical Neuroanatomy

journal homepage: www.elsevier.com/locate/jchemneu

Distribution of histaminergic neuronal cluster in the rat and mouse hypothalamus

Chinatsu Moriwaki [a], Seiichi Chiba [a,*], Huixing Wei [a,b], Taishi Aosa [a,b], Hirokazu Kitamura [a], Keisuke Ina [a], Hirotaka Shibata [b], Yoshihisa Fujikura [a]

[a] Department of Molecular Anatomy, Faculty of Medicine, Oita University, Japan
[b] Department of Endocrinology, Metabolism, Rheumatology and Nephrology, Faculty of Medicine, Oita University, Japan

ARTICLE INFO

Article history:
Received 27 April 2015
Received in revised form 11 June 2015
Accepted 1 July 2015
Available online 9 July 2015

Keywords:
Rat
Mouse
Hypothalamus
Histidine decarboxylase
Histamine
Neuron

ABSTRACT

Histidine decarboxylase (HDC) catalyzes the biosynthesis of histamine from l-histidine and is expressed throughout the mammalian nervous system by histaminergic neurons. Histaminergic neurons arise in the posterior mesencephalon during the early embryonic period and gradually develop into two histaminergic substreams around the lateral area of the posterior hypothalamus and the more anterior peri-cerebral aqueduct area before finally forming an adult-like pattern comprising five neuronal clusters, E1, E2, E3, E4, and E5, at the postnatal stage. This distribution of histaminergic neuronal clusters in the rat hypothalamus appears to be a consequence of neuronal development and reflects the functional differentiation within each neuronal cluster. However, the close linkage between the locations of histaminergic neuronal clusters and their physiological functions has yet to be fully elucidated because of the sparse information regarding the location and orientation of each histaminergic neuronal clusters in the hypothalamus of rats and mice. To clarify the distribution of the five-histaminergic neuronal clusters more clearly, we performed an immunohistochemical study using the anti-HDC antibody on serial sections of the rat hypothalamus according to the brain maps of rat and mouse. Our results confirmed that the HDC-immunoreactive (HDCi) neuronal clusters in the hypothalamus of rats and mice are observed in the ventrolateral part of the most posterior hypothalamus (E1), ventrolateral part of the posterior hypothalamus (E2), ventromedial part from the medial to the posterior hypothalamus (E3), periventricular part from the anterior to the medial hypothalamus (E4), and diffusely extended part of the more dorsal and almost entire hypothalamus (E5). The stereological estimation of the total number of HDCi neurons of each clusters revealed the larger amount of the rat than the mouse. The characterization of histaminergic neuronal clusters in the hypothalamus of rats and mice may provide useful information for further investigations.

Abbreviations: 3V, 3rd ventricle; Arc, arcuate hypothalamic nucleus; ArcD, arcuate hypothalamic nucleus, dorsal part; ArcL, arcuate hypothalamic nucleus, lateral part; ArcM, arcuate hypothalamic nucleus, medial part; ArcMP, arcuate hypothalamic nucleus, medial posterior part; ArcLP, arcuate hypothalamic nucleus, lateroposterior part; DM, dorsomedial hypothalamic nucleus; DMC, dorsomedial hypothalamic nucleus, compact part; DMD, dorsomedial hypothalamic nucleus, dorsal part; DMV, dorsomedial hypothalamic nucleus, ventral part; DTM, dorsal tuberomammillary nucleus; f, fornix; fr, fasciculus retroflexus; LH, lateral hypothalamic area; MRe, mammillary recess of the 3rd ventricle; mp, mammillary peduncle; mt, mammillothalamic tract; PBP, parabrachial pigmented nucleus of the VTA; Pe, periventricular hypothalamic nucleus; PH, posterior hypothalamic nucleus; PHA, posterior hypothalamic area; PLH, peduncular part of the lateral hypothalamus; pm, principal mammillary tract; PMD, premammillary nucleus, dorsal part; PMV, premammillary nucleus, ventral part; SNCD, dorsal tier of the compact part of substantia nigra; SNR, reticular part of substantia nigra; Spa, subparaventricular zone of the hypothalamus; TuLH, tuberal region of lateral hypothalamus; VTA, ventral tegmental area; VTAR, rostral part of ventral tegmental area; VTM, ventral tuberomammillary nucleus; ZI, zona incerta; ZID, zona incerta, dorsal part; ZIV, zona incerta, ventral part.

* Corresponding author at: Department of Molecular Anatomy, Faculty of Medicine, Oita University 1-1, Idaigaoka, Yufu-city, Oita 879-5593, Japan.
E-mail address: schiba@oita-u.ac.jp (S. Chiba).

http://dx.doi.org/10.1016/j.jchemneu.2015.07.001
0891-0618/

1. Introduction

Neuronal histamine in the mammalian hypothalamus is synthesized from l-histidine by histidine decarboxylase (HDC) in the histaminergic neurons (Haas et al., 2008; Panula et al., 2014) consists of HDC-containing nerve cells with multitudinous varicose dendrites and axons, and is involved in various cerebral functions such as the circadian rhythms, wakefulness, feeding behavior, thermogenesis, neuroendocrine regulation, mood, memory, learning, and cognitive performance (Dere et al., 2003; Haas et al., 2008; Parmentier et al., 2002; Provensi et al., 2014; Sakata et al., 2003; Wada et al., 1991; Yoshimatsu et al., 2002; Yu et al., 2014). The development of histaminergic neurons is characterized as follows; histamine-immunoreactive neurons are detected first at the border of the mesencephalon and the metencephalon at embryonic day 13; on both sides of the midline on the ventral side of the cerebral aqueduct; and on the caudal side of the pons at embryonic day 16, and they were observed in the caudal, tuberal, and postmammillary caudal nuclei in the posterior hypothalamus at embryonic day 20, while the histaminergic neurons in the mesencephalon and myelencephalon completely disappear by this embryonic day (Auvinen and Panula, 1988; Vanhala et al., 1994). On the first postnatal day, histamine-immunoreactive neurons appear in all three magnocellular subnuclei, namely the caudal, tuberal, and postmammillary caudal magnocellular nuclei and around the ventromedial and dorsomedial hypothalamic nuclei. The distribution of histamine-immunoreactive neurons in these nuclei attains an adult-like appearance at postnatal day 20 (Auvinen and Panula, 1988). In particular, histamine-immunoreactive neurons developed from the border area between mesencephalon and metencephalon, showed two streams of the lateral area of the posterior hypothalamus and peri-cerebral aqueduct area (Panula et al., 1988). These two substreams of histamine-immunoreactive neurons appeared to develop into several subclusters comprising the histaminergic nervous system of adult vertebrates (Haas et al., 2008; Molina-Hernandez et al., 2012). The adult rat exhibits five subgroups of HDC-immunoreactive neuronal clusters in the hypothalamus, namely E1, E2, and E3 in the posterior hypothalamic area; E4 in the ventromedial hypothalamic area; and E5 in more dorsal part of the hypothalamus in a diffusely scattered pattern (Inagaki et al., 1990). In the rodent hypothalamus, histaminergic neuronal clusters are grouped in five clusters, E1–E5, each of which sends overlapping projections throughout the neuroaxis with a low level of topographical organization, and are bridged by scattered neurons (Ericson et al., 1987; Inagaki et al., 1990). The former three subclusters E1–E3 appear to develop from the border area between mesencephalon and metencephalon, and the latter two subclusters E4–E5 develop from the peri-cerebral aqueduct area of the diencephalon (Auvinen and Panula, 1988; Haas et al., 2008; Molina-Hernandez et al., 2012; Vanhala et al., 1994; Watanabe et al., 1984). The manner of the histaminergic neuron development in rats and mice shares a high degree of similarity despite a relatively short developmental period in mice (Nissinen et al., 1995; Nissinen and Panula, 1995). Understanding this distribution of histaminergic clustering in the hypothalamus is likely to be important for further physiological studies of the histaminergic nervous system of mammals (Blandina et al., 2012). However, there is an urgent need to compare the hypothalamic distribution of the five-histaminergic neuronal clusters in rats and mice because of the scarcity of data with respect to precise depictions by common rodent brain maps. The intractable nature of hypothalamic histaminergic neuronal cluster nomenclature has further complicated histaminergic research and hindered our ability to contextualize research findings, particularly from studies involving mice (Inagaki et al., 1990; Karlstedt et al., 2001; Michelsen and Panula, 2002; Miklos and Kovacs, 2003; Puelles et al., 2012; Sunkin et al., 2013; Umehara et al., 2010, 2011, 2012).

In the present study, we conducted an immunohistochemical investigation to examine the hypothalamic orientations of five histaminergic neuronal clusters of rats and mice in an aim to contribute to further research in the relationship between physiological regulation and the distribution of histaminergic neuronal clusters in the mammalian hypothalamus.

2. Materials and methods

2.1. Animals

In this study, 10 male Wistar rats and 10 male 57Bl/6 mice with initial weights of approximately 290 g and 26–30 g about 10 weeks according to previous reports (Table 1), respectively, were used. Four animals were housed per cage in a soundproof room under a 12-h/12-h light/dark cycle (lights on at 07:00) and fed a standard laboratory diet and tap water ad libitum. All procedures were performed in accordance with the Oita University Guide for the Care and Use of Laboratory Animals, which is based on the National Institutes of Health guidelines, and were approved by the Animal Care Committee of Oita University.

2.2. Chemicals

For light microscopic immunohistochemistry, a rabbit polyclonal antibody to full length histidine decarboxylase without cross-reactivity to DOPA decarboxylase of rat and mouse (HDC; 1/2000, PROGEN Inc., Heidelberg, Germany) (Dartsch et al., 1999), a rabbit IgG (Santa Cruz Biotechnology, Inc., Dallas, USA), the EnVision System (antirabbit IgG-HRP conjugated, Dako Inc., Copenhagen, Denmark), bovine serum albumin (BSA; Sigma Aldrich Chem., St. Louis, USA), and 3,3′-diaminobenzidine 4HCl (DAB; Wako Pure Chemical Industries, Ltd, Osaka, Japan) were used.

2.3. Experimental procedures

All animals were anesthetized at 10:00 with pentobarbital sodium (150 mg/kg i.p.) and perfused through the left ventricle with ice-cold saline followed by 4% paraformaldehyde in 0.05 M Cacodylate buffer (pH 7.4). Brains were removed, placed in fixative overnight, and then dehydrated with ethyl alcohol series before embedding in paraffin. Frontal serial sections were cut at a thickness of 10 μm and fixed to MAS-coated glass slides (Matsunami Glass Ind. Ltd., Osaka, Japan). Sections

Table 1
Determination of histaminergic neuronal clusters of HDC-positive neurons.

Inagaki et al. (1990)	Ericson et al. (1987)	Köhler et al. (1985)	Staines et al. (1987)	Bleier et al. (1979)
Wistar, m	SD, m	SD, m	SD, m	HA, f
E1	TMVc	TMv	Ps	CMc
E2	TMVr	TMv	Ls	CMr
E3	TMMv	TMv	Vs	N.D.
E4	TMMd	TMdm	Ts	TM
E5	TMdiff	TMdif	Is	N.D.

The first row represents corresponding author in classification; the second row: rat name and gender; and the third to seventh row: subgroup names for each study. Wistar: represents Wistar rats; SD: Sprague–Dawley rats; HA: Höltzman albino rats; m: male, and f: female: TMVc and TMVr: caudal and rostral parts of ventral subgroup of the TM, respectively: TMMv and the TMMd; ventral and dorsal part of medial subgroup of TM, TMdiff: the diffuse part of the TM, respectively: TMv, TMdm, and TMdif: ventral, dorsomedial, and diffuse parts of the TM, respectively: Ps: posterior subdivision of postmammillary caudal magnocellular nucleus: Ls: the lateral subdivision of the caudal magnocellular nucleus: Vs: the ventral subdivision of a cell group at the base of the hypothalamus between the arcuate nucleus (Arc) and the premammillary nucleus, which continues caudally within the peripheral borders of the mammillary body: Ts: the subdivision of a tightly gathered cluster near to the third ventricle, rostrally, or the mammillary recess, caudally: Is: the interstitial subdivision of a field of dispersed cells found at anterior levels of the tuberomammillary nucleus: CMc: the caudal part of the caudal magnocellular nucleus: CMr: the rostral part of the caudal magnocellular nucleus: TM: the tuberal magnocellular nucleus: N.D.: not determined.

were deparaffinized in xylene and immersed in methanol with H_2O_2 for 30 min at 4 °C and then hydrated in a series of descending ethanol concentrations before being immersed in running tap water for 5 min. Subsequently, sections were incubated in 1% BSA in PBS (BSA–PBS; 0.01 M phosphate buffer + 0.15 M NaCl, pH 7.2) for 30 min at room temperature (RT) and then incubated in rabbit IgG anti-HDC (1/2000) overnight at 4 °C. Serial sections were then rinsed in BSA–PBS for 30 min at RT before use of the Envision System (for 2 h) and DAB visualization (for 10 min) at RT to detect HDC immunoreactivity (HDCi). All sections were counterstained with hematoxylin. The specificity of the HDC antibody was confirmed by performing the same procedure described above with the use of a rabbit IgG (Santa Cruz Biotechnology, Inc., Dallas, USA) instead of the primary rabbit polyclonal antibody to HDC (PROGEN Inc., Heidelberg, Germany).

2.4. Nomenclature of HDC-immunoreactive neuronal clusters

We evaluated serial sections of the entire rat hypothalamus to confirm the distribution of HDCi neuronal clusters as previously reported (Table 1). All serial section evaluations were conducted according to the rat brain map (Paxinos and Watson, 2005) and the mouse brain map (Franklin and Paxinos, 2008) for rat and mouse studies, respectively. The E1 neuronal cluster (Inagaki et al., 1990) corresponds to histaminergic neurons found in the caudal region of the ventral subgroup of TM (TMVc) (Ericson et al., 1987), ventral region of TM (TMv) (Köhler et al., 1985), posterior subdivision of the caudal magnocellular nucleus (Ps) (Staines et al., 1987), and caudal region of the caudal magnocellular nucleus (CMc) (Bleier et al., 1979). The E2 neuronal cluster (Inagaki et al., 1990) corresponds to the rostral region of ventral subgroup of TM (TMVr) (Ericson et al., 1987), TMv (Köhler et al., 1985), lateral subdivision of the caudal magnocellular nucleus (Ls) (Staines et al., 1987), and rostral region of the caudal magnocellular nucleus (CMr) (Bleier et al., 1979). The E3 neuronal cluster (Inagaki et al., 1990) corresponds to the ventral region of the medial subgroup of TM (TMMv) (Ericson et al., 1987), TMv (Köhler et al., 1985), and ventral subdivision of a cell group at the base of the hypothalamus between the arcuate nucleus and premammillary nucleus that caudally continues within the peripheral borders of the mammillary body (Vs) (Staines et al., 1987). The E4 neuronal cluster (Inagaki et al., 1990) corresponds to the dorsal region of the medial subgroup of TM (TMMd) (Ericson et al., 1987), dorsomedial part of TM (TMdm) (Köhler et al., 1985), subdivision of a tightly gathered cluster adjacent to the third ventricle rostrally or mammillary recess caudally (Ts) (Staines et al., 1987), and tuberal magnocellular nucleus (TM) (Bleier et al., 1979). The E5 neuronal cluster (Inagaki et al., 1990) corresponds to a diffuse region of TM (TMdiff) (Ericson et al., 1987), a diffuse region of TM (TMdif) (Köhler et al., 1985), and the interstitial subdivision of a field of dispersed cells found at the anterior levels of the tuberomammillary nucleus, which is the only cell group not constituting a distinct cell cluster (Is) (Staines et al., 1987). The diameters of each neuron within the histaminergic clusters were measured according to the scale bars of individual light microscopy images, and recorded as mean values ± standard error of the mean (SEM) (μm). Clusters were defined as regions containing over 95% HDCi neurons with the broken line in photomicrograph images.

2.5. Stereological estimation of the total number of HDC-immunoreactive neurons

Stereological counting methods were used to obtain an accurate estimate of the number of HDC-immunoreactive neurons of each cluster. Serial coronal sections (10 μm) were made through the hypothalamus, and every 20th section was saved and digitized spanning bregma −1.08 to −4.68 for rat, and −0.34 to −2.92 for mouse. Only cells that displayed prominent nuclear profiles were scored in the same side of the hypothalamus. The total number of HDC-immunoreactive cell profiles was estimated by the following formula:

$$N_{\text{total}} = \frac{(t \cdot f) \cdot \sum_{i=1}^{n} Q_i}{t}$$

where N_{total} is the total number of HDC-immunoreactive cell profiles, section thickness $t = 10$ μm, $f = 20$, Q_i = counted cell profiles in the uniformly sampled dissectors (crude number), and $n = 10$ (number of equidistant sections used in the analysis) for E1, $n = 11$ for E2, $n = 22$ for E3, $n = 24$ for E4, and $n = 33$ for E5 of rats; $n = 5$ for E1, $n = 7$ for E2, $n = 11$ for E3, $n = 17$ for E4, and $n = 22$ for E5 of mice, respectively. The calculated distance from one section to the next was 200 μm. The number of cells in each of the 1st to ith sampled sections was used to calculate the coefficient of error (Hains et al., 2003; Sasaki et al., 2009; Smolen et al., 1983).

2.6. Statistical analysis

Statistics are expressed as mean ± SEM. Continuous variables were compared by the analysis of variance (ANOVA). Statistical significance was set at $P < 0.05$. All calculations were performed with SAS software (JMP 11.0, SAS Institute, Cary, NC, USA).

3. Results

3.1. Distribution of HDCi neurons according to nomenclature of the hypothalamic histaminergic neuronal clusters of rat

Fig. 1 shows the sections between −1.20 mm and −4.68 mm from the bregma. Numerical values of the diameters of each rat HDCi neuronal cluster according to the rat brain map (Paxinos and Watson, 2005) are presented in Table 2. In the −1.20-mm section from the bregma (Fig. 1A), the rostral site of the hypothalamus, HDCi neuronal clusters comprising medium-sized cells were observed around the subparaventricular zone of the hypothalamus (SPa) and the periventricular hypothalamic nucleus (Pe) (Table 2). The area around SPa and Pe was identified as the most rostral region of E4. In addition, HDCi neuronal cluster containing relatively large cells that were found around the peduncular part of the lateral hypothalamic area (PLH) was confirmed as the most rostral region of E5 (E5r) (Table 2). Furthermore, this HDCi neuronal cluster was identified at a homologous site within PLH of mice slightly rostral to PLH in the −1.20-mm rat section from the bregma (PLH, Table 3). In the −1.80-mm section from the bregma (Fig. 1B), E4 medial region was clearly observed around Pe rather than around Spa (Table 3). In the −2.76-mm section from the bregma (Fig. 1C), the most rostral region of E3 comprising small-sized cells was observed around the medial part of the arcuate hypothalamic nucleus (ArcM, Table 2), and the dorsomedial region of E4 was observed around Pe and dorsal part of the dorsomedial

Table 2
The variances of the diameters of five histaminergic neuronal clusters of rats and mice.

	Rats	Mice
E1	$38.91 \pm 2.07^{**,\dagger}$	$25.01 \pm 0.81^{**,\dagger}$
E2	$37.69 \pm 1.24^{**,\dagger}$	$25.36 \pm 0.44^{**,\dagger}$
E3	$16.10 \pm 0.50^{*}$	$18.46 \pm 0.16^{*}$
E4	$18.08 \pm 0.55^{*}$	$18.01 \pm 0.14^{*}$
E5	$23.09 \pm 0.77^{*,**}$	$23.06 \pm 0.16^{*,**}$

Numerical data was shown in mean ± SEM. The left column represented the name of each histaminergic neuronal clusters, the middle column exhibited the results of rats, and the right the results of mice.
* $P < 0.05$ vs E1 and E2.
** $P < 0.05$ vs E3 and E4.
† $P < 0.05$ vs the same cluster between rats and mice.

Table 3
Contiguous nuclei around HDCi neuronal clusters of rats.

Rat brain map	E1	E2	E3	E4	E5
Bregma −1.08				Pe/Spa	(PLH)
Bregma −1.20				Pe/Spa	PLH
Bregma −1.56				Pe/Spa	PLH
Bregma −1.80				Pe/Spa	PLH/TuLH
Bregma −2.04				Pe/Spa	PLH/TuLH
Bregma −2.28				Pe/DMD	PLH/TuLH
Bregma −2.52				Pe/DMD	PLH/TuLH
Bregma −2.76			ArcM/ArcD	Pe/DMD	PLH/TuLH
Bregma −3.00			ArcM/ArcD	Pe/DMD	PLH/TuLH
Bregma −3.24			ArcM/ArcD	Pe/DMD	PLH/TuLH
Bregma −3.48			ArcMP/ArcLP	Pe/DMD	PLH/TuLH/PH
Bregma −3.72		VTM	ArcMP/ArcLP	DTM/DM	PLH/PMV/PH
Bregma −3.96		VTM	ArcMP/ArcLP		PLH/PMD/PMV/PH
Bregma −4.20		VTM	ArcMP/ArcLP		PLH/PH
Bregma −4.44		VTM			PLH/PHA
Bregma −4.68	VTM				PHA

The left column represented the numerical distance (mm) from the bregma according to brain map (Paxinos and Watson, 2005); the other columns, the name of each histaminergic neuronal clusters. SPa: the subparaventricular zone of the hypothalamus, Pe: the periventricular hypothalamic nucleus, PLH: the peduncular part of the lateral hypothalamic area, TuLH: the tuberal region of lateral hypothalamus, DMD: the dorsal part of the dorsomedial hypothalamic nucleus, ArcM: the medial part of the arcuate hypothalamic nucleus, ArcD: the dorsal part of the arcuate hypothalamic nucleus, PH: the posterior hypothalamic nucleus, ArcMP: the medial posterior part of the arcuate hypothalamic nucleus, ArcLP: the lateroposterior part of the arcuate hypothalamic nucleus, DM: the dorsomedial hypothalamic nucleus, DTM: the dorsal part of the tuberomammillary nucleus, VTM: the ventral tuberomammillary nucleus, PMV: the ventral part of the premammillary nucleus, PMD: the dorsal part of the premammillary nucleus, PHA: the posterior hypothalamic area. The term (PLH) indicated the homologous site of PLH of mice just at more rostral site to PLH of rats.

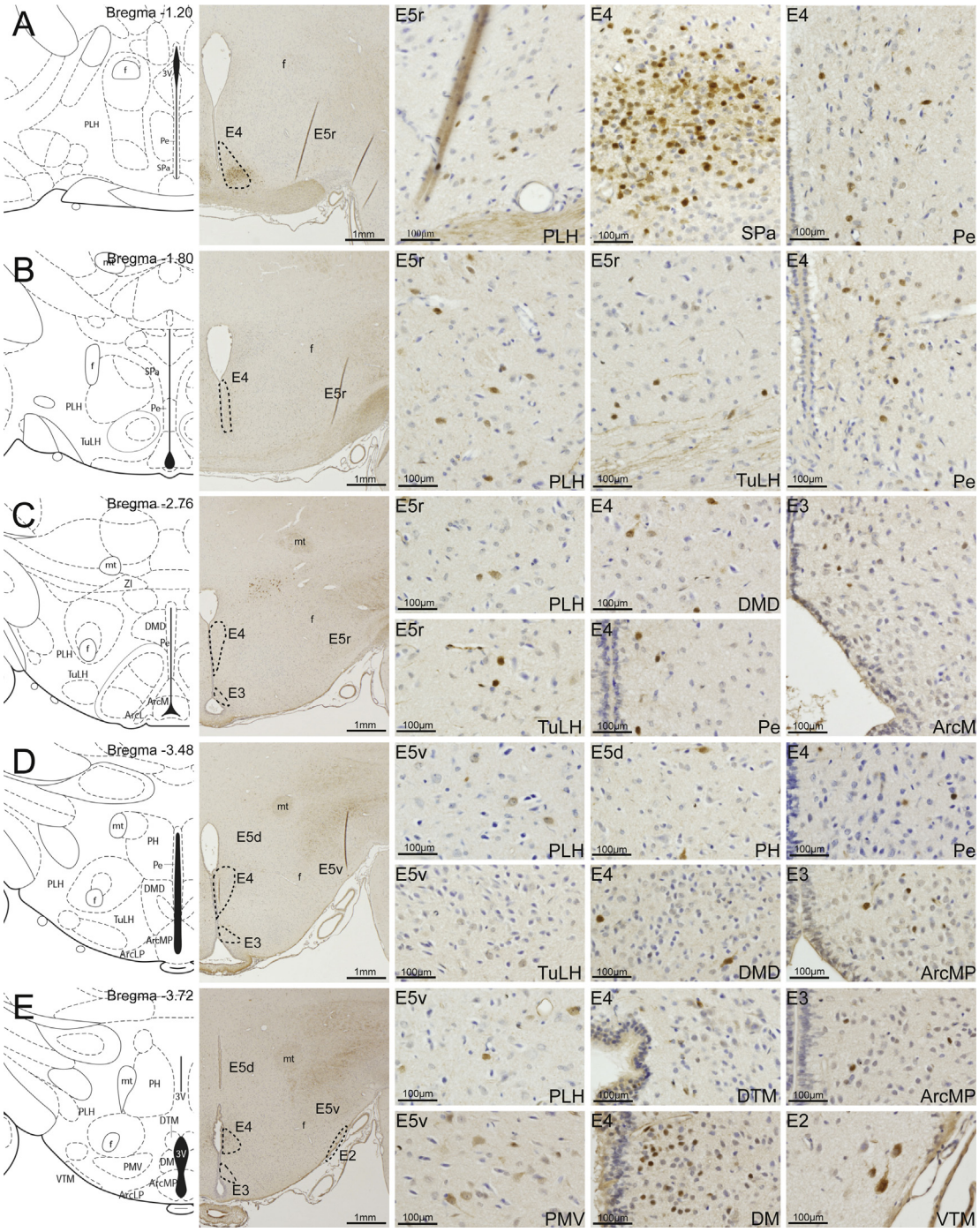

Fig. 1. HDCi neuronal clusters of the hypothalamus of rats. The first column represented schemas of brain map of rat; the second, the low-power field photomicrographs of the hypothalamus of rat (×20); the other columns, the high-power field photomicrographs of the counterpart area to brain map (×200). Each row contained the distance numerically (mm) from the bregma at the right upper site of the first row according to brain map. The browny HDCi neurons were categorized to five neural clusters; E1, E2, E3, and E4 by broken lines; E5 by the open area around the correspondent neural nuclei represented in each schema. The subclusters of E5 were represented as E5r the rostral part, E5v the ventral part, and E5d the dorsal part of E5, respectively. Scale bars were indicated at the lower site of all photomicrographs. The other abbreviations; SPa: the subparaventricular zone of the hypothalamus, Pe: the periventricular hypothalamic nucleus, PLH: the peduncular part of the lateral hypothalamic area, TuLH: the tuberal region of lateral hypothalamus, DM: the dorsomedial hypothalamic nucleus, DMD: the dorsal part of the dorsomedial hypothalamic nucleus, ArcM: the medial part of the arcuate hypothalamic nucleus, ZI: the zona incerta of the thalamus, PH: the posterior hypothalamic nucleus, ArcLP: the lateroposterior part of the arcuate hypothalamic nucleus, ArcMP: the medial posterior part of the arcuate hypothalamic nucleus, DTM: the dorsal part of the tuberomammillary nucleus, VTM: the ventral tuberomammillary nucleus, PMV: the ventral part of the premammillary nucleus, PMD: the dorsal part of the premammillary nucleus, PHA: the posterior hypothalamic area, SNR: the reticular part of substantia nigra, VTAR: the rostral part of ventral tegmental area, VTA: the ventral tegmental area, PBP: the parabrachial pigmented nucleus of the VTA, SNCD: the dorsal tier of the compact part of substantia nigra, MRe: the mammillary recess of the 3rd ventricle, 3V: 3rd ventricle, f: fornix, mt: mammillothalamic tract, mp: mammillary peduncle.

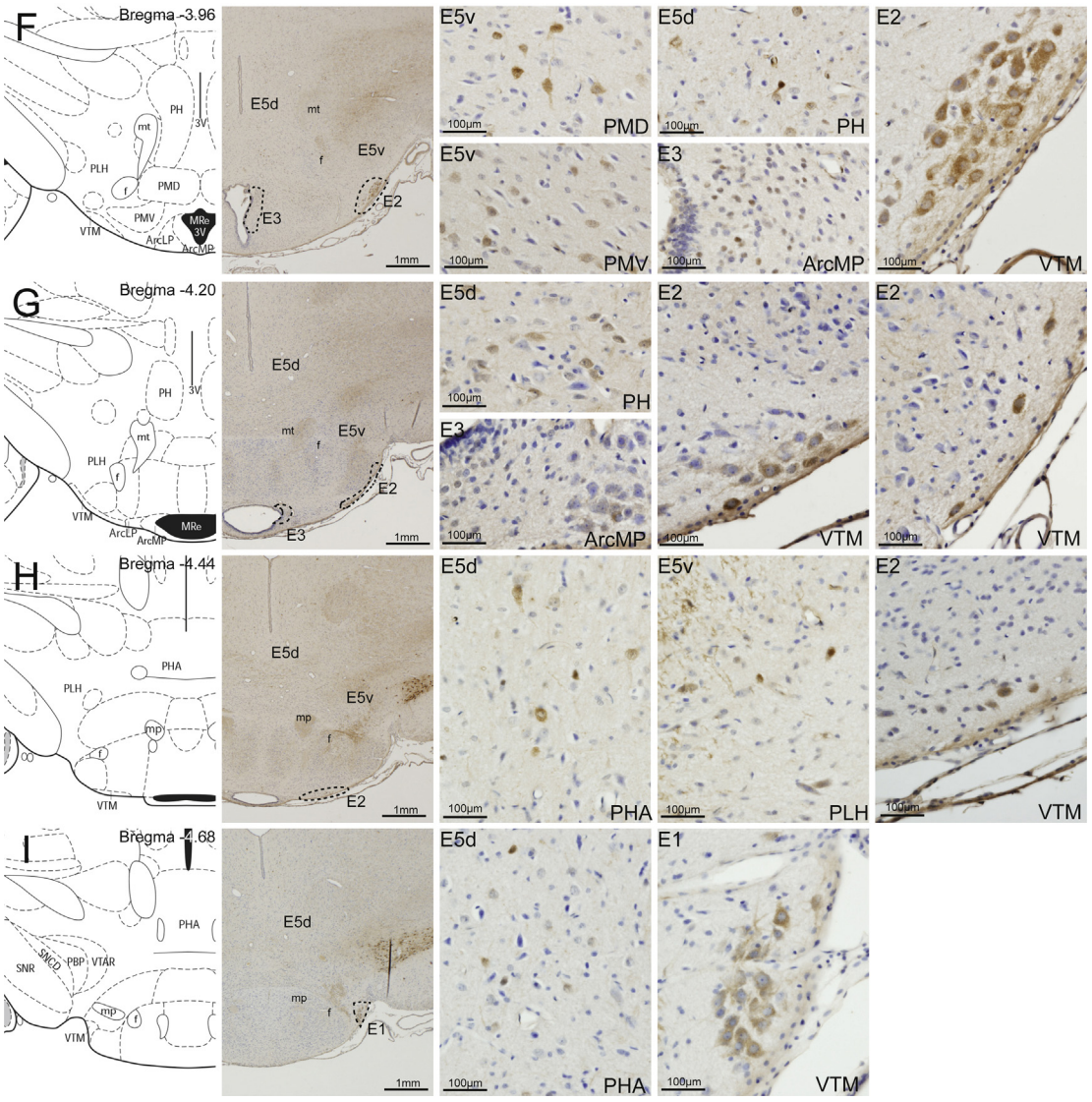

Fig. 1. (*Continued*).

hypothalamic nucleus (DMD). The rostral region of E5 (E5r) was observed around PLH and the tuberal region of the lateral hypothalamus (TuLH) (Table 3). In the −3.48-mm section from the bregma (Fig. 1D), the dorsal region of E5 (E5d) was around the posterior hypothalamic nucleus (PH) and the ventral region of E5 (E5v) was observed in a diffuse continuation from TuLH and PLH. The medial region of E4 was around Pe and the dorsal part of DMD. The medial posterior part of the arcuate hypothalamic nucleus (ArcMP), continuing to the ArcM, was observed as the medial region of E3 (Table 3). In the −3.72-mm section from the bregma (Fig. 1E), the most rostral region of E2 comprising large-sized cells was observed around the medial part of the ventral tuberomammillary nucleus (VTM, Table 2), and the medial region of E3 was observed around ArcMP; the most dorso-caudal and ventral region of E4 were observed around the dorsal tuberomammillary nucleus (DTM) and the ventral part of the dorsomedial hypothalamic nucleus (DMV) leading to the DMD. The medial region of E5v was also observed around the ventral part of the premammillary nucleus (PMV) leading to TuLH (Table 3). In the −3.96-mm section from the bregma (Fig. 1F), the medial region of E5v was observed around the dorsal part of the premammillary nucleus (PMD) and PMV (Table 3). In the −4.20-mm section from the bregma (Fig. 1G), the most caudal region of E3 was observed around the ArcMP. The most rostral region of E1 comprising large-sized cells was observed around the lateral region of VTM (Table 2). Moreover, the caudal region of E2 was observed around the medial region of VTM. The caudal regions of E5d and E5v were observed around PH and seen bridging to PLH (Table 3). In the −4.44-mm section from the bregma (Fig. 1H), the most caudal region of E5d was observed around the posterior hypothalamic area (PHA) leading to PH with the lateral region of E5v also found around PLH (Table 3). The most caudal region of E2 was observed around the medial region of VTM (Table 3). In the −4.68-mm section from the bregma (Fig. 1I), the most caudal regions of E1 and E5d were observed around the lateral region of VTM and PHA (Table 3). The divergence of E5r to E5v and E5d was rostrally observed in sections −1.08 mm to −4.68 mm from the bregma, covering almost the entire hypothalamus (Table 3). In this study, HDCi neuronal cluster was less frequently observed in the preoptic area (POA), suprachiasmatic nucleus (SCN), paraventricular hypothalamic nucleus (PVN), and ventromedial hypothalamic nucleus (VMH).

These observations can be summarized from the most caudal to the most rostral as follows. E1 is predominantly comprised of large-sized cells with a mean diameter of 38.91 ± 2.07 μm (Table 2) and is located at the ventrolateral site of the posterior hypothalamus (Table 3). E2 is comprised of large-sized cells with a mean diameter of

37.69 ± 1.24 μm (Table 2) and is located between −3.72 to −4.44 mm from the bregma most caudally at the ventromedial site and most rostrally at the ventrolateral site of the posterior hypothalamus (Table 3). E3 is predominantly comprised of small-sized cells with a mean diameter of 16.10 ± 0.50 μm (Table 2) and is located between −2.76 and −4.20 mm from the bregma most caudally around the lateral site to ArcMP near MRe at the ventromedial site and most rostrally around the lateral site to ArcM at the ventrolateral region of the medio-posterior hypothalamus (Table 3). E4 is comprised of relatively small-sized cells with a mean diameter of 18.08 ± 0.55 μm (Table 2) and is located between −1.08 and −3.72 mm from the bregma and located most caudally around DM and DTM near the third ventricle and most rostrally around Pe and SPa at the medial site of the antero-medial hypothalamus (Table 3). E5 is comprised of medium-sized cells with a mean diameter of 23.09 ± 0.77 μm (Table 2) and is located between −1.08 and −4.68 mm from the bregma most caudally around PHA at the most dorsomedial site of the posterior hypothalamus and most rostrally around PLH and TuLH at the dorsolateral site of the anterior hypothalamus (Table 3). No statistically significant difference in cell diameter was observed among the three E5 subclusters. The estimated total numbers of HDC-immunoreactive neurons of each cluster were $4120 \pm 348^{*}$ for E1, $2680 \pm 200^{*}$ for E2, $5840 \pm 232^{*,**}$ for E3, $22{,}820 \pm 1526^{**}$ for E4, and $17{,}160 \pm 341^{**}$ for E5 of the rat ($^{*}p < 0.05$ vs rat E5, $^{**}p < 0.05$ vs rat E1); $380 \pm 42^{\dagger}$ for E1, $1400 \pm 63^{\dagger}$ for E2, $5000 \pm 297^{\dagger}$ for E3, $13{,}680 \pm 499^{\dagger}$ for E4, and $22{,}040 \pm 271^{\dagger}$ for E5 of the mouse ($\dagger p < 0.05$ vs every cluster of the mouse). The estimated order of the total number of HDCi neurons of each cluster in rats and mice can be represented as follows: E1 = E2 < E3 < E4 = E5 for the rat; E1 < E2 < E3 < E4 < E5 for the mouse.

In addition, we observed the HDCi neuronal clusters in extra-hypothalamic locations; HDCi stainings were identified at the thalamus, including the zona incerta (ZI) (Fig. 1C, Table S1), the rostral part (VTAR), and the parabrachial pigmented nucleus of the ventral tegmental area (PBP), and the reticular part (SNR), the dorsal tier of the compact part of substantia nigra (SNCD) (Fig. 1H and I, Table S1), and the striatum (data was not shown).

3.2. Distribution of HDCi neurons according to nomenclature of the hypothalamic histaminergic neuronal clusters of mouse

Fig. 2 shows serial sections between −0.34 mm and −2.92 mm from the bregma. Numerical values for the diameters of individual mouse HDCi neuronal clusters according to the mouse brain map (Franklin and Paxinos, 2008) are presented in Table 2. In the −0.34-mm section from the bregma (Fig. 2A) representing the most rostral site of the hypothalamus, HDCi neuronal clusters were observed around PLH and Pe. The area around Pe comprising medium-sized cells was identified as the most rostral region of E4 (Table 2). The area around PLH comprising large-sized cells was confirmed as the most rostral region of E5 (E5r, Table 2). Contiguous HDCi neuronal clusters were observed from −0.34 (Fig. 2A) to −0.58 mm from the bregma (Table 4). In the −0.70-mm section from the bregma (Fig. 2B), the medial region of E4 was observed around Pe and SPa and extended to −0.94 mm from the bregma (Table 4). In the −1.06-mm section from the bregma (Fig. 2C), the rostral region of E5 (E5r) was around PLH and TuLH. In addition, the medial region of E4 was observed around Pe but not Spa (Table 4). In the −1.22-mm section from the bregma (Fig. 2D), the most rostral region of E3 comprising small-sized cells (Table 2) was observed around the arcuate hypothalamic nucleus (Arc, Table 4). In the −1.34-mm section from the bregma (Fig. 2E), the medial and dorsal regions of E4, both comprising medium-sized cells (Table 2), were observed around DM and Pe and could be followed to −2.30 mm from the bregma (Fig. 2K, Table 4). E5r was observed around PLH but not TuLH (Fig. 2E, Table 4). Moreover, E5r was observed around PLH (Table 4). In the −1.46-mm section from the bregma (Fig. 2F), E4 and E5 were consecutively observed around Pe as well as DM and around PLH, respectively (Table 4). The E3 subgroup around Arc appeared to bridge between the third

Table 4
Contiguous nuclei around HDCi neuronal clusters of mice.

Mouse brain map	E1	E2	E3	E4	E5
Bregma −0.34				Pe	PLH
Bregma −0.46				Pe	PLH
Bregma −0.58				Pe	PLH
Bregma −0.70				Pe/Spa	PLH
Bregma −0.82				Pe/Spa	PLH
Bregma −0.94				Pe/Spa	PLH
Bregma −1.06				Pe	PLH/TuLH
Bregma −1.22			Arc	Pe	PLH/TuLH
Bregma −1.34			Arc	Pe/DM	PLH
Bregma −1.46			Arc	Pe/DM	PLH
Bregma −1.58			Arc	Pe/DM	PLH
Bregma −1.70			ArcD/ArcL	Pe/DM	PLH
Bregma −1.82			ArcD/ArcL	Pe/DMD/DMV/DMC	PLH
Bregma −1.94			ArcD/ArcL	Pe/DMD/DMV/DMC	PLH
Bregma −2.06			ArcD/ArcL/ArcM	DM/DMC	PLH/PH
Bregma −2.18		VTM	ArcMP/ArcLP	DM	LH/PH
Bregma −2.30		VTM	ArcMP/ArcLP	DM/DTM	LH/PH/PMV
Bregma −2.46		VTM	ArcMP/ArcLP	DTM	LH/PH/PMV/PMD
Bregma −2.54		VTM	ArcMP/ArcLP	DTM	LH/PH/PMV/PMD
Bregma −2.70		VTM	ArcMP		PH/PMD
Bregma −2.80	VTM	VTM			(PHA)
Bregma −2.92	VTM	VTM			(PHA)

The left column represented the numerical distance (mm) from the bregma according to brain map (Franklin and Paxinos, 2008); the other columns, the name of each histaminergic neuronal clusters. SPa: the subparaventricular zone of the hypothalamus, Pe: the periventricular hypothalamic nucleus, PLH: the peduncular part of the lateral hypothalamic area, TuLH: the tuberal region of lateral hypothalamus, Arc: the arcuate hypothalamic nucleus, DM: the dorsomedial hypothalamic nucleus, DMD: the dorsal part of the dorsomedial hypothalamic nucleus, ArcM: the medial part of the arcuate hypothalamic nucleus, PH: the posterior hypothalamic nucleus, LH: the lateral hypothalamic area, ArcD: the dorsal part of the arcuate hypothalamic nucleus, ArcL: the lateral part of the arcuate hypothalamic nucleus, ArcMP: the medial posterior part of the arcuate hypothalamic nucleus, ArcLP: the lateroposterior part of the arcuate hypothalamic nucleus, DTM: the dorsal part of the tuberomammillary nucleus, VTM: the ventral tuberomammillary nucleus, PMV: the ventral part of the premammillary nucleus, PMD: the dorsal part of the premammillary nucleus, PHA: the posterior hypothalamic area. The term (PHA) indicated the homologous site of PHA of rats just at more caudal site to PH of mice.

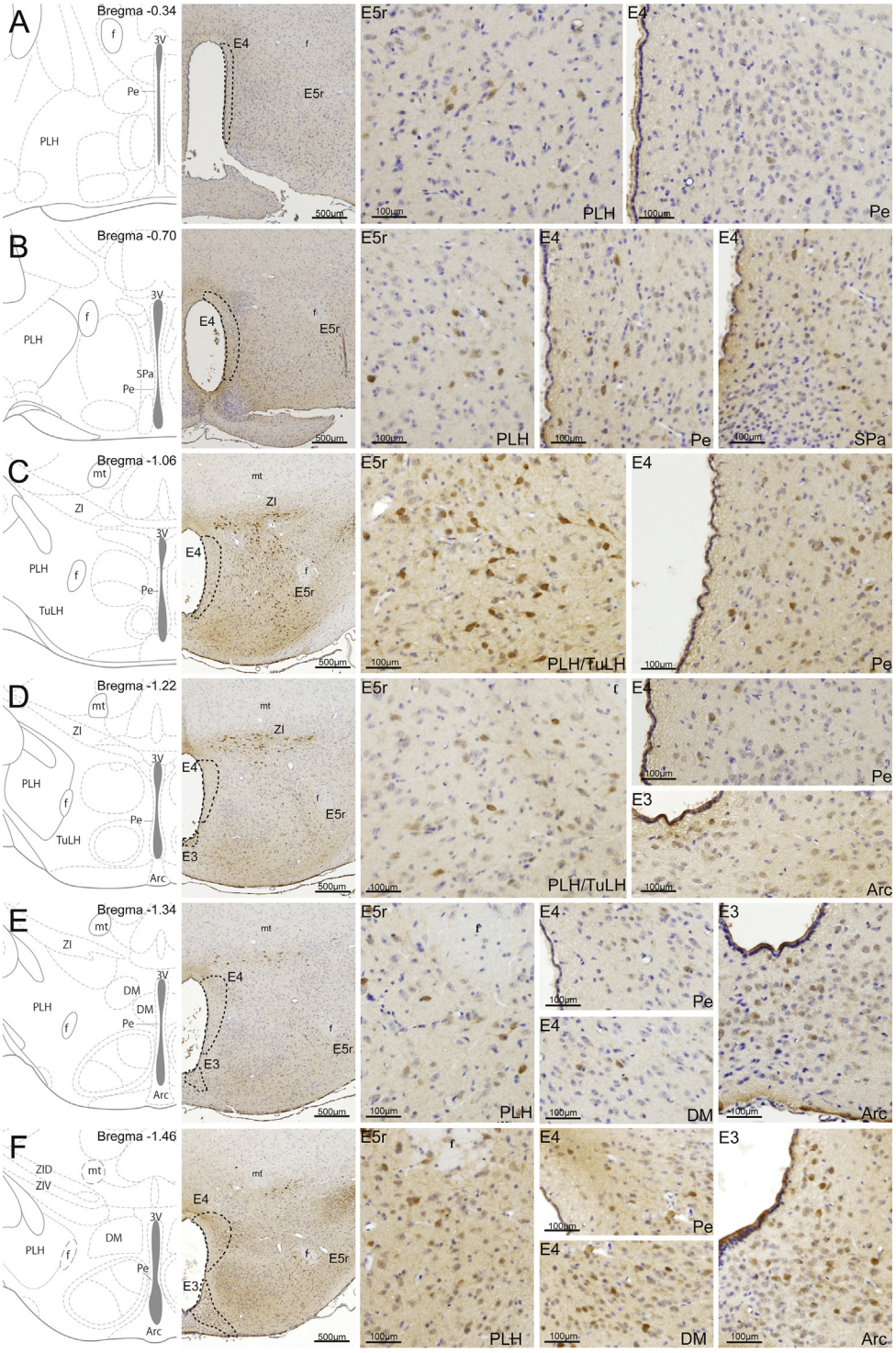

Fig. 2. HDCi neuronal clusters of the hypothalamus of mice. The first column represented schemas of brain map of mouse; the second, the low-power field photomicrographs of the hypothalamus of mouse (×40); the other columns, the high-power field photomicrographs of the counterpart area to brain map (×200). Each row contained the distance numerically (mm) from the bregma at the right upper site of the first row according to brain map. The browny HDCi neurons were categorized to five neural clusters; E1, E2, E3, and E4 by broken lines; E5 by the open area around the correspondent neural nuclei represented in each schema. The subclusters of E5 were represented as E5r the rostral part, E5v the ventral part, and E5d the dorsal part of E5, respectively. Scale bars were indicated at the lower site of all photomicrographs. The other abbreviations; SPa: the subparaventricular zone of the hypothalamus, Pe: the periventricular hypothalamic nucleus, PLH: the peduncular part of the lateral hypothalamic area, TuLH: the tuberal region of lateral hypothalamus, Arc: the arcuate hypothalamic nucleus, DM: the dorsomedial hypothalamic nucleus, DMD: the dorsal part of the dorsomedial hypothalamic nucleus, DMV: the ventral part of the dorsomedial hypothalamic nucleus, DMC: the compact part of the dorsomedial hypothalamic nucleus, ArcM: the medial part of the arcuate hypothalamic nucleus, ZI: the zona incerta of the thalamus, ZID: the dorsal part of the zona incerta, ZIV: the ventral part of zona incerta, PH: the posterior hypothalamic nucleus, LH: the lateral hypothalamic area, ArcD: the dorsal part of the arcuate hypothalamic nucleus, ArcL: the lateral part of the arcuate hypothalamic nucleus, ArcLP: the lateroposterior part of the arcuate hypothalamic nucleus, ArcMP: the medial posterior part of the arcuate hypothalamic nucleus, DTM: the dorsal part of the tuberomammillary nucleus, VTM: the ventral tuberomammillary nucleus, PMV: the ventral part of the premammillary nucleus, PMD: the dorsal part of the premammillary nucleus, PHA: the posterior hypothalamic area, SNR: the reticular part of substantia nigra, VTAR: the rostral part of ventral tegmental area, VTA: the ventral tegmental area, PBP: the parabrachial pigmented nucleus of the VTA, SNCD: the dorsal tier of the compact part of substantia nigra, MRe: the mammillary recess of the 3rd ventricle, 3V: 3rd ventricle, f: fornix, mt: mammillothalamic tract, pm: principal mammillary tract, fr: fasciculus retroflexus. The term of (PHA) in O and P; a homologous site of PHA of rat.

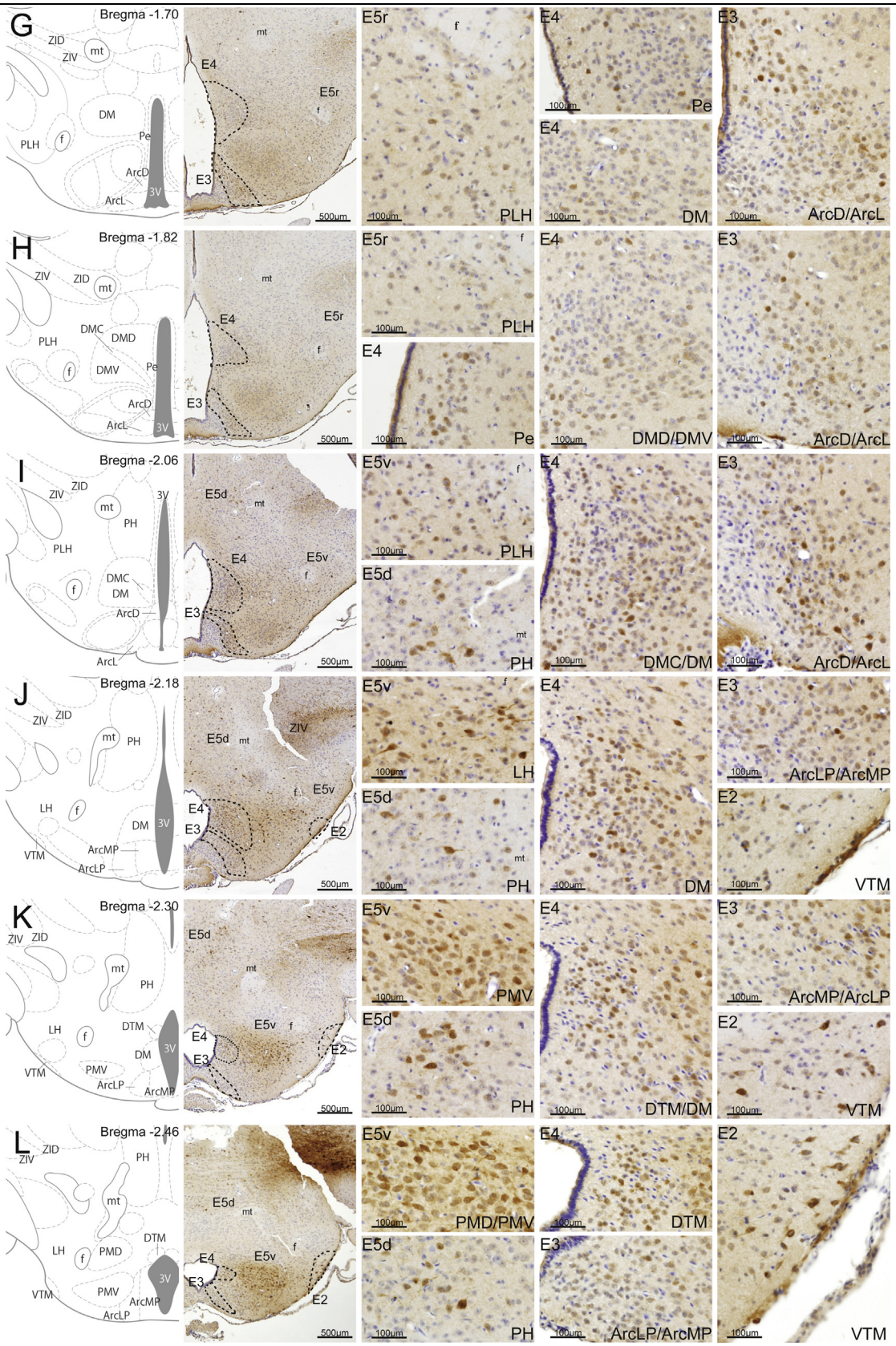

Fig. 2. (*Continued*)

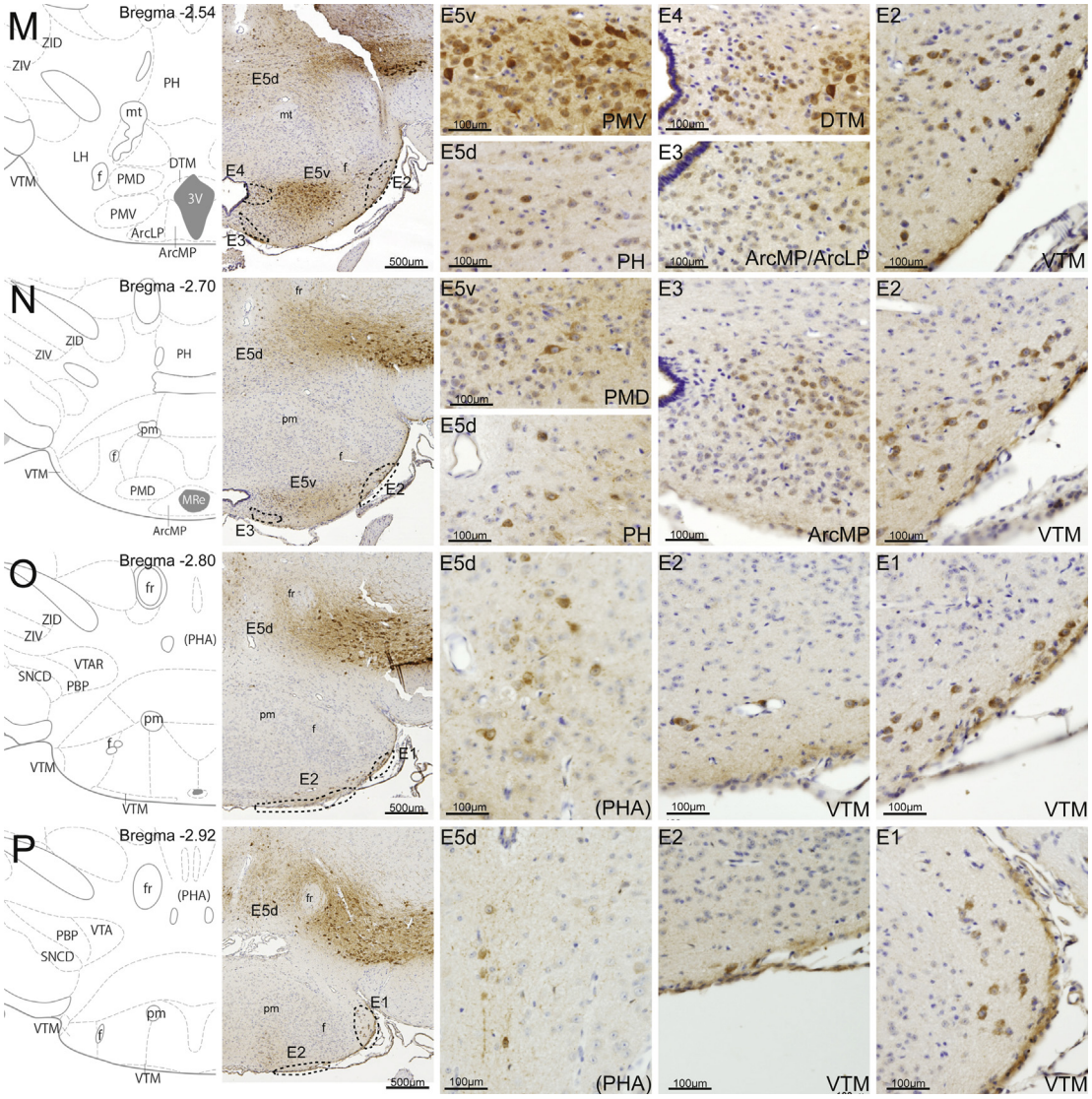

Fig. 2. (*Continued*).

ventricle and ventral surface of the hypothalamus. In the −1.70-mm section from the bregma (Fig. 2G), the medial region of E3 was observed around the dorsal part of the arcuate hypothalamic nucleus (ArcD) and the lateral part of the arcuate hypothalamic nucleus (ArcL, Table 4). In the −1.82-mm section from the bregma (Fig. 2H), the medial and dorsal regions of E4 were observed around Pe, dorsal part of DMD, and ventral part of the dorsomedial hypothalamic nucleus (DMV, Table 4). In the −2.06-mm section from the bregma (Fig. 2I), the dorsal region of E5 (E5d) was observed around PH. The ventral region of E5 (E5v) continued in a diffuse pattern from E5r to PLH and the medial and dorsal regions of E4 continued from DMD and DMV to DM. This divergence of E5r into E5v and E5d was rostrally observed from the −2.06-mm section from the bregma continuing almost to the caudal site of the hypothalamus (Fig. 2I, Table 4). In the −2.18-mm section from the bregma (Fig. 2J), the caudal region of E5v, continuing from PLH, was observed around the lateral hypothalamic area (LH) and the medial region of E3, leading to ArcD and ArcL, was observed around the medial posterior part of ArcMP and the lateroposterior part of the arcuate hypothalamic nucleus (ArcLP). The most rostral region of E2, comprising large-sized cells (Table 2) was observed around the medial region of VTM (Table 4). In the −2.30-mm section from the bregma (Fig. 2K), the dorsal region of E4 was observed around DM and DTM, and the most medial region of E5v was around the ventral region of PMV (Table 4). In the −2.46-mm section from the bregma (Fig. 2L), the medial region of E5v was around the dorsal region of PMD near to PMV. In the −2.54-mm section from the bregma (Fig. 2M), the most caudal region of E4 was around DTM (Table 4). In the −2.70-mm section from the bregma (Fig. 2N), the most caudal region of E5v was around PMD and the most caudal region of E3 was around the ArcMP (Table 4). In the −2.80-mm section from the bregma (Fig. 2O), the most rostral region of E1, comprising large-sized cells (Table 2), was around the lateral region of VTM (Table 4). In the −2.92-mm section from the bregma (Fig. 2P), the most caudal region of E2 was around the medial site of VTM, and the most caudal region of E1 was around the lateral site of VTM (Table 4). HDCi neuronal clusters around the dorsomedial region of posterior hypothalamus leading to PH in mice (Fig. 2N), a site homologous with PHA in rats (PHA, Fig. 1H and I), appeared to represent the most caudal region of E5d (Fig. 2O and P, Table 4).

These observations can be summarized from caudal to rostral as follows.

E1 is predominantly comprised of large-sized cells with a mean diameter of 25.01 ± 0.81 μm (Table 2) and is located between −2.80 mm and −2.92 mm from the bregma at the ventrolateral site of the posterior hypothalamus (Table 4). E2 is comprised of large-sized

cells with a mean diameter of 25.36 ± 0.44 μm (Table 2) and is located between −2.18 mm and −2.92 mm from the bregma most caudally at the ventromedial site and most rostrally at the ventrolateral site of the posterior hypothalamus (Table 4). E3 is predominantly comprised of small-sized cells with a mean diameter of 18.46 ± 0.16 μm (Table 2) and is located between −1.22 mm and −2.70 mm from the bregma most caudally around ArcMP near MRe at the ventromedial site and most rostrally around Arc at the ventrolateral site of the medio-posterior hypothalamus (Table 4). E4 is constituted by relatively small-sized cells with a mean diameter of 18.01 ± 0.14 μm (Table 2) and is located between −0.34 mm and −2.54 mm from the bregma most caudally adjacent to DTM near the third ventricle and most rostrally around Pe at the medial site of the antero-medial hypothalamus (Table 4). E5 is comprised of medium-sized cells with a mean diameter of 23.06 ± 0.16 μm (Table 2) and is located between −0.34 mm and −2.70 mm from the bregma most caudally around PMD at the most dorsomedial site of the posterior hypothalamus and most rostrally around PLH at the dorsolateral site of the anterior hypothalamus (Table 4). Schematic figures of sagittal planes of hypothalamic HDCi neuronal clusters of the rat (Supplemental Fig. 1A) and the mouse (Supplemental Fig. 1B) according to brain maps (Franklin and Paxinos, 2008; Paxinos and Watson, 2005) are also available to see an overview of the location of the five HDCi neuronal clusters in comparison of the rat with the mouse.

In addition, we observed HDCi neuronal clusters in extra-hypothalamic regions; HDCi staining was identified in the thalamus, including ZI (Fig. 2C–E, Table S2), the dorsal part of the zona incerta, and the ventral part of the zona incerta (Fig. 2F–O, Table S2), VTAR and PBP, the dorsal tier of the substantia nigra pars compacta (Fig. 2O and P, Table S2), and the striatum in a similar pattern to that observed in rats (data not shown).

Table 2 also shows variances in the diameters of the five-histaminergic neuronal clusters in rats and mice. A significant difference in the mean diameters of clusters E1 and E2 compared with other clusters was observed with a significant difference of E5 and clusters E3 and E4 were also observed (Table 2). A significant difference in mean neuron diameter was observed between clusters with the same coding of the clusters between rats and mice were detected for E1 and E2 (Table 2). The mean neuron diameters of these clusters in rats and mice can be ranked as follows: E1 = E2 > E5 > E3 = E4.

4. Discussion

HDC staining of serial sections clearly demonstrated the distribution of HDCi neuronal clusters, E1, E2, E3, E4, and E5, according to Inagaki's nomenclature (Table 1). Herein, we present comprehensive outline of the histaminergic neuronal clusters in rats and mice in detailed photomicrographs (Figs. 1 and 2, Suppl. Fig. 1), summarized lists (Tables 2–4), and estimated the total number of HDC-immunoreactive neurons of each clusters using stereological quantification. E1 (Inagaki et al., 1990), the caudal region of the ventral subgroup of the tuberomammillary nucleus (TMVc) (Ericson et al., 1987), was observed in the most ventrolateral site of the posterior hypothalamus, as a cluster of large neurons. E2 (Inagaki et al., 1990), the rostral region of the ventral subgroup of the tuberomammillary nucleus (TMVr) (Ericson et al., 1987), was observed in the most ventromedial site of the posterior hypothalamus, as a cluster of large neurons. Whereas neurons of E1 and E2 were almost identical in size and found in close proximity, a clear discontinuation was observed between E1 and E2 clusters (Figs. 1E–I and 2J–P, Tables 2–4). This observation does not contradict previous suggestions that E1 and E2 are distinct nuclei with differing roles in behavior reinforcement in rats (Wagner et al., 1993). E3 (Inagaki et al., 1990), the ventral region of the medial subgroup of the tuberomammillary nucleus (TMMv) (Ericson et al., 1987), was observed in the most medial site around the third ventricle of the middle part of the hypothalamus as a cluster of small neurons. E4 (Inagaki et al., 1990), the dorsal region of the medial subgroup of the tuberomammillary nucleus (TMMd) (Ericson et al., 1987), was observed in the dorsal site around the third ventricle from the anterior to the relative posterior area of the hypothalamus as a cluster of small neurons. Whereas neurons of E3 and E4 were almost identical in size and in close proximity, a clear distinction between E3 and E4 clusters was observed with the range of E4 obviously greater along with the third ventricle as compared with that of E3 (Figs. 1E and I, 2J and P, Tables 2–4). E5 (Inagaki et al., 1990), the diffuse region of the tuberomammillary nucleus (TMdiff) (Ericson et al., 1987), was observed in the most extended site, between the antero-lateral site and the posterior site across the hypothalamus as a cluster of medium-sized neurons. E5 around PLH (Figs. 1C and 2H) appeared to be further divided into another two substreams, the postero-dorsal substream around PH (Figs. 1D–I and 2I–P) and postero-ventral substream around PM and PLH (Figs. 1D–I and 2I–N). To make this observation more clear, we attempted to divide the E5 cluster into three subclusters; the rostral region of E5 (E5r) (Figs. 1A–C and 2A–H), the dorsal aspect of the caudal region of E5 (E5d) (Figs. 1D–I and 2I–P), and the ventral aspect of the caudal region of E5 (E5v) (Figs. 1D–H and 2I–N). The estimation of total number of HDCi neurons of each clusters exhibiting the larger amount of rat compared to mouse may reflect the difference of body mass between these rodents. Moreover, the most major subgroups among the HDCi neuronal clusters were E5 and E4 for the rat, and E5 for the mouse, whereas the most minor subgroups were E1 and E2 for the rat, and E1 for the mouse. These differences may yield to the stereological distribution of these clusters (Figs. 1 and 2, Suppl. Fig. 1).

Our present study was subject to some limitations in the research design. Although this study aimed to depict the precise location of histaminergic neuronal clusters in rats and mice, detailed assessments of innervations nor physiological roles of histaminergic clusters were not investigated. Despite these limitations, the present findings, particularly in detailing the regions of E4 and E5 in rats and mice are quite available and provide a rationale for further evaluation of the relationship between HDCi neuronal clusters and nearby neuronal nuclei in the examination for the various physiological studies of the histaminergic neuronal system.

As the figures and tables for E5 in rats and mice demonstrate (Figs. 1 and 2, Tables 3 and 4), the peduncular part of the lateral hypothalamus (PLD) and the tuberal part of the lateral hypothalamus (TuLH) were identified adjacent to the rostral region of E5 (E5r), and these nuclei have been shown to be involved in the hypothalamic–pituitary–gonadal axis (Ayala et al., 2013), GABAA-dependent feeding behavior (Turenius et al., 2009), and hypoglycemia-induced feeding behavior via orexin (Griffond et al., 1999). Therefore, the ventral part (PMV) and dorsal part (PMD) of the premammillary nuclei were also found nearby to the ventral aspect of the caudal region of E5 (E5v) (Figs. 1 and 2, Tables 3 and 4), and these nuclei have been shown to participate in the reproductive functions (Cavalcante et al., 2014; Furigo et al., 2014; Nagaishi et al., 2014) and the regulation of maternal mood and behavior (Litvin et al., 2014; Motta et al., 2013). The posterior hypothalamic nucleus (PH) and the posterior hypothalamic area (PHA) were observed adjacent to the dorsal aspect of caudal region of E5 (E5r), and these nuclei have been shown to contribute to stress-management in association with melanin-concentrating hormone (MCH) and orexin (Flak et al., 2012; Hahn, 2010) and the nociceptive management (Gavrilov et al., 2008; Matsuzaki et al., 2015). Because histaminergic receptors are widely distributed among these nuclei (Haas et al., 2008), it has been suggested that

E5r may contribute to the regulation of feeding behaviors and gonadal functions, E5v to the reproductions and maternal behaviors, and E5d to the nociceptive response. Furthermore, the histaminergic neuronal clusters of E5 around lateral hypothalamic nuclei may integrate signals involved in regulation of the arousal state via the orexin pathway because of the observation that E5 neurons co-express orexin type B receptor (Gerashchenko et al., 2004). In summary, E5 appears to chiefly be involved in regulation of seasonal reproduction and stress coping in strong association with orexin.

E4 in rats and mice, as shown in the figures and tables (Figs. 1 and 2, Tables 3 and 4), was observed broadly around the dorsal site of the third ventricle, involving among most rostrally the periventricular hypothalamic nucleus (Pe), the ventral part of the subparaventricular zone of the hypothalamus (Spa), the dorsal part (DMD), the ventral part (DMV), the compact part (DMC) of the dorsomedial hypothalamic nucleus (DM), and the dorsal tuberomammillary nucleus (DTM), the most caudal region of E4. Pe is known for signal transduction in hypoxia (Huang et al., 2007), chronic mild stress (Kim et al., 2003), galanin (Takatsu et al., 2001), hypothalamic–pituitary–gonadal axis via somatostatin by GABAA (Bingaman et al., 1994; Llorens-cortes et al., 1992), and thyrotropin-releasing hormone by the glucocorticoid receptor (Cintra et al., 1990), respectively. The Spa has substantial roles in the relayed pathway from the suprachiasmatic nucleus (SCN) to DM with participation of orexin neurons (Nakamura et al., 2008; Schwartz et al., 2009; Yoshida et al., 2006) and integration of circadian rhythms (Phillips et al., 2013; Saper et al., 2005). DM, receiving dense efferents from SCN via Spa, is now noted for the critical role in the central regulation of the brown adipose tissues (BAT) for energy homeostasis in mammals (Kataoka et al., 2014; Nakamura and Morrison, 2011), particularly via central leptin signaling (Enriori et al., 2011; Rezai-Zadeh et al., 2014). The DTM, a classical subnucleus of histaminergic neurons, is noted for an important role in the regulation of arousal (Castillo-Ruiz et al., 2013) through signal transduction of the acid-sensing ion channels (ASICs) for brain chemosensation (Meng et al., 2009), melanin-concentration hormone (MCH) for memory formation (Casatti et al., 2002), and neuropeptide S for wakefulness (Zhao et al., 2012). In summary, E4 appears to be predominantly involved in the regulation of circadian rhythms of energy metabolism in strong association with diurnal control of the SCN-DM-BAT sympathetic pathway.

E3 in rats and mice, as demonstrated in the figures and tables (Figs. 1 and 2, Tables 3 and 4), was observed throughout the lateral region of the arcuate hypothalamic nucleus (Arc), known to express histaminergic receptors (Haas et al., 2008), at the ventromedial site of the hypothalamus. Arc is a critical center of feeding behavior in response to hunger sensation and has been suggested to be under the control of the histaminergic E3 neuronal cluster (Umehara et al., 2012). In summary, E3 may be involved in diurnal energy-osmoregulation because of the role of E3 in drinking behavior and urination (Mahia et al., 2007a, 2009) and the innervation of orexin (Torrealba et al., 2003).

E2 in rats and mice, as demonstrated in the figures and tables (Figs. 1 and 2, Tables 3 and 4), was observed as a medial region of the ventral tuberomammillary nucleus (VTM) at the ventromedial site of the caudal hypothalamus. The neuronal cluster of E2, clearly distinct from the E1 cluster by its physiological role (Wagner et al., 1993), has well-documented roles in the feeding regulation (Mahia et al., 2007b), sensing of hypercapnia (Haxhiu et al., 2001; Johnson et al., 2005), integration of the somatomotor and cardiosympathetic functions (Krout et al., 2003), memory formation and reinforcement (Huston et al., 1997; Wagner et al., 1993), and involvement of immune-sensory pathways (Gaykema et al., 2008) in association with arousal regulation (Castillo-Ruiz et al., 2013) via orexin (Bayer et al., 2001) and neuropeptide S (Zhao et al., 2012). In summary, E2 is considered a key cluster integrating behavioral modifications with arousal enhancement between the five-histaminergic neuronal clusters.

E1 in rats and mice, as demonstrated in the figures and tables (Figs. 1 and 2, Tables 3 and 4), was observed as the most caudal region of VTM. The neuronal cluster of E1, overlapping with many physiological roles of E2, may participate in the physiological regulation of pineal gland due to the demonstration of histaminergic innervation of the pineal gland from the E1 neuronal cluster (Mikkelsen et al., 1992). In summary, E1 is a cluster reported to functionally shift circadian regulation to a greater degree than E2 (I'Anson et al., 2011), whereas these two clusters appear to be organized into a single functional complex. Moreover, extrahypothalamic HDCi neuronal clusters were also observed around the basal ganglia corroborating previous studies (Ito et al., 1996; Krusong et al., 2011; Pollard et al., 1985; Rozov et al., 2014).

There have been few reported studies comparing the distribution of HDCi neuronal clusters in the hypothalamus of rats and mice, particularly in E4 and E5 using orientation with standard brain maps. In the present study, we localize the five HDCi neuronal clusters of rats and mice using popular brain maps and, despite some limitations, believe this report will serve as an available valuable orientation tool for many future studies of the histaminergic nervous system in the mammalian hypothalamus.

Conflict of interest

None.

All authors of this paper declare that there is no conflict of interest related to the content of this manuscript, including employment or personal financial interests.

Ethical statement

All experiments were performed in accordance with the Oita University Guide for the Care and Use of Laboratory Animals, which is based on the National Institutes of Health guidelines, and were approved by the Animal Care Committee of Oita University.

Acknowledgments

We are grateful to Mr. Shuji Tatsukawa and Ms. Yukari Goto for their help with all studies. We respectfully dedicate this manuscript to the late Hironobu Yoshimatsu, a distinguished professor of Oita University.

Appendix A. Supplementary data

Supplementary data associated with this article can be found, in the online version, at http://dx.doi.org/10.1016/j.jchemneu.2015.07.001.

References

Auvinen, S., Panula, P., 1988. Development of histamine-immunoreactive neurons in the rat brain. J. Comp. Neurol. 276, 289–303.

Ayala, C., Pennacchio, G.E., Soaje, M., Carreno, N.B., Bittencourt, J.C., Jahn, G.A., Celis, M.E., Valdez, S.R., 2013. Effects of thyroid status on NEI concentration in specific brain areas related to reproduction during the estrous cycle. Peptides 49, 74–80.

Bayer, L., Eggermann, E., Serafin, M., Saint-Mleux, B., Machard, D., Jones, B., Muhlethaler, M., 2001. Orexins (hypocretins) directly excite tuberomammillary neurons. Eur. J. Neurosci. 14, 1571–1575.

Bingaman, E.W., Baeckman, L.M., Yracheta, J.M., Handa, R.J., Gray, T.S., 1994. Localization of androgen receptor within peptidergic neurons of the rat forebrain. Brain Res. Bull. 35, 379–382.

Blandina, P., Munari, L., Provensi, G., Passani, M.B., 2012. Histamine neurons in the tuberomamillary nucleus: a whole center or distinct subpopulations? Front. Syst. Neurosci. 6, 33.

Bleier, R., Cohn, P., Siggelkow, I., 1979. A Cytoarchitectonic Atlas of the Hypothalamus and Hypothalamic Third Ventricle of the Rat. Marcel Dekker, NY, USA.
Casatti, C.A., Elias, C.F., Sita, L.V., Frigo, L., Furlani, V.C., Bauer, J.A., Bittencourt, J.C., 2002. Distribution of melanin-concentrating hormone neurons projecting to the medial mammillary nucleus. Neuroscience 115, 899–915.
Castillo-Ruiz, A., Gall, A.J., Smale, L., Nunez, A.A., 2013. Day–night differences in neural activation in histaminergic and serotonergic areas with putative projections to the cerebrospinal fluid in a diurnal brain. Neuroscience 250, 352–363.
Cavalcante, J.C., Bittencourt, J.C., Elias, C.F., 2014. Distribution of the neuronal inputs to the ventral premammillary nucleus of male and female rats. Brain Res. 1582, 77–90.
Cintra, A., Fuxe, K., Wikstrom, A.C., Visser, T., Gustafsson, J.A., 1990. Evidence for thyrotropin-releasing hormone and glucocorticoid receptor-immunoreactive neurons in various preoptic and hypothalamic nuclei of the male rat. Brain Res. 506, 139–144.
Dartsch, C., Sundler, F., Persson, L., 1999. Antisera against rat recombinant histidine decarboxylase: immunocytochemical studies in different species. Histochem. J. 31, 507–514.
Dere, E., De Souza-Silva, M.A., Topic, B., Spieler, R.E., Haas, H.L., Huston, J.P., 2003. Histidine-decarboxylase knockout mice show deficient nonreinforced episodic object memory, improved negatively reinforced water-maze performance, and increased neo- and ventro-striatal dopamine turnover. Learn. Mem. 10, 510–519.
Enriori, P.J., Sinnayah, P., Simonds, S.E., Garcia Rudaz, C., Cowley, M.A., 2011. Leptin action in the dorsomedial hypothalamus increases sympathetic tone to brown adipose tissue in spite of systemic leptin resistance. J. Neurosci. 31, 12189–12197.
Ericson, H., Watanabe, T., Köhler, C., 1987. Morphological analysis of the tuberomammillary nucleus in the rat brain: delineation of subgroups with antibody against L-histidine decarboxylase as a marker. J. Comp. Neurol. 263, 1–24.
Flak, J.N., Solomon, M.B., Jankord, R., Krause, E.G., Herman, J.P., 2012. Identification of chronic stress-activated regions reveals a potential recruited circuit in rat brain. Eur. J. Neurosci. 36, 2547–2555.
Franklin, K., Paxinos, G., 2008. The Mouse Brain in Stereotaxic Coordinates, 3rd ed. Elsevier Academic Press, MA, USA.
Furigo, I.C., Kim, K.W., Nagaishi, V.S., Ramos-Lobo, A.M., de Alencar, A., Pedroso, J.A., Metzger, M., Donato Jr., J., 2014. Prolactin-sensitive neurons express estrogen receptor-alpha and depend on sex hormones for normal responsiveness to prolactin. Brain Res. 1566, 47–59.
Gavrilov, Y.V., Perekrest, S.V., Novikova, N.S., 2008. Intracellular expression of c-Fos protein in various structures of the hypothalamus in electrical pain stimulation and administration of antigens. Neurosci. Behav. Physiol. 38, 87–92.
Gaykema, R.P., Park, S.M., McKibbin, C.R., Goehler, L.E., 2008. Lipopolysaccharide suppresses activation of the tuberomammillary histaminergic system concomitant with behavior: a novel target of immune-sensory pathways. Neuroscience 152, 273–287.
Gerashchenko, D., Chou, T.C., Blanco-Centurion, C.A., Saper, C.B., Shiromani, P.J., 2004. Effects of lesions of the histaminergic tuberomammillary nucleus on spontaneous sleep in rats. Sleep 27, 1275–1281.
Griffond, B., Risold, P.Y., Jacquemard, C., Colard, C., Fellmann, D., 1999. Insulin-induced hypoglycemia increases preprohypocretin (orexin) mRNA in the rat lateral hypothalamic area. Neurosci. Lett. 262, 77–80.
Haas, H.L., Sergeeva, O.A., Selbach, O., 2008. Histamine in the nervous system. Physiol. Rev. 88, 1183–1241.
Hahn, J.D., 2010. Comparison of melanin-concentrating hormone and hypocretin/orexin peptide expression patterns in a current parceling scheme of the lateral hypothalamic zone. Neurosci. Lett. 468, 12–17.
Hains, B.C., Black, J.A., Waxman, S.G., 2003. Primary cortical motor neurons undergo apoptosis after axotomizing spinal cord injury. J. Comp. Neurol. 462, 328–341.
Haxhiu, M.A., Tolentino-Silva, F., Pete, G., Kc, P., Mack, S.O., 2001. Monoaminergic neurons, chemosensation and arousal. Respir. Physiol. 129, 191–209.
Huang, J., Tamisier, R., Ji, E., Tong, J., Weiss, W.J., 2007. Chronic intermittent hypoxia modulates nNOS mRNA and protein expression in the rat hypothalamus. Respir. Physiol. Neurobiol. 158, 30–38.
Huston, J.P., Wagner, U., Hasenohrl, R.U., 1997. The tuberomammillary nucleus projections in the control of learning, memory and reinforcement processes: evidence for an inhibitory role. Behav. Brain Res. 83, 97–105.
I'Anson, H., Jethwa, P.H., Warner, A., Ebling, F.J., 2011. Histaminergic regulation of seasonal metabolic rhythms in Siberian hamsters. Physiol. Behav. 103, 268–278.
Inagaki, N., Toda, K., Taniuchi, I., Panula, P., Yamatodani, A., Tohyama, M., Watanabe, T., Wada, H., 1990. An analysis of histaminergic efferents of the tuberomammillary nucleus to the medial preoptic area and inferior colliculus of the rat. Exp. Brain Res. 80, 374–380.
Ito, C., Onodera, K., Sakurai, E., Sato, M., Watanabe, T., 1996. The effect of methamphetamine on histamine level and histidine decarboxylase activity in the rat brain. Brain Res. 734, 98–102.
Johnson, P.L., Moratalla, R., Lightman, S.L., Lowry, C.A., 2005. Are tuberomammillary histaminergic neurons involved in CO2-mediated arousal? Exp. Neurol. 193, 228–233.
Karlstedt, K., Nissinen, M., Michelsen, K.A., Panula, P., 2001. Multiple sites of L-histidine decarboxylase expression in mouse suggest novel developmental functions for histamine. Dev. Dyn. 221, 81–91.
Kataoka, N., Hioki, H., Kaneko, T., Nakamura, K., 2014. Psychological stress activates a dorsomedial hypothalamus-medullary raphe circuit driving brown adipose tissue thermogenesis and hyperthermia. Cell Metab. 20, 346–358.
Kim, H., Whang, W.W., Kim, H.T., Pyun, K.H., Cho, S.Y., Hahm, D.H., Lee, H.J., Shim, I., 2003. Expression of neuropeptide Y and cholecystokinin in the rat brain by chronic mild stress. Brain Res. 983, 201–208.
Köhler, C., Swanson, L.W., Haglund, L., Wu, J.Y., 1985. The cytoarchitecture, histochemistry and projections of the tuberomammillary nucleus in the rat. Neuroscience 16, 85–110.
Krout, K.E., Mettenleiter, T.C., Loewy, A.D., 2003. Single CNS neurons link both central motor and cardiosympathetic systems: a double-virus tracing study. Neuroscience 118, 853–866.
Krusong, K., Ercan-Sencicek, A.G., Xu, M., Ohtsu, H., Anderson, G.M., State, M.W., Pittenger, C., 2011. High levels of histidine decarboxylase in the striatum of mice and rats. Neurosci. Lett. 495, 110–114.
Litvin, Y., Cataldo, G., Pfaff, D.W., Kow, L.M., 2014. Estradiol regulates responsiveness of the dorsal premammillary nucleus of the hypothalamus and affects fear- and anxiety-like behaviors in female rats. Eur. J. Neurosci. 40, 2344–2351.
Llorens-cortes, C., Bertherat, J., Jomary, C., Kordon, C., Epelbaum, J., 1992. Regulation of somatostatin synthesis by GABAA receptor stimulation in mouse brain. Brain Res. Mol. Brain Res. 13, 277–281.
Mahia, J., Bernal, A., Garcia Del Rio, C., Puerto, A., 2009. The natriuretic effect of oxytocin blocks medial tuberomammillary polydipsia and polyuria in male rats. Eur. J. Neurosci. 29, 1440–1446.
Mahia, J., Bernal, A., Puerto, A., 2007a. Dipsogenic potentiation by sodium chloride but not by sucrose or polyethylene glycol in tuberomammillary-mediated polydipsia. Exp. Brain Res. 183, 27–39.
Mahia, J., Bernal, A., Puerto, A., 2007b. Hyperphagia and increased body weight induced by lesions of the ventral tuberomammillary system. Behav. Brain Res. 181, 147–152.
Matsuzaki, K., Katakura, M., Inoue, T., Hara, T., Hashimoto, M., Shido, O., 2015. Aging attenuates acquired heat tolerance and hypothalamic neurogenesis in rats. J. Comp Neurol. Comp. Neurol. 523, 1190–1201.
Meng, Q.Y., Wang, W., Chen, X.N., Xu, T.L., Zhou, J.N., 2009. Distribution of acid-sensing ion channel 3 in the rat hypothalamus. Neuroscience 159, 1126–1134.
Michelsen, K.A., Panula, P., 2002. Subcellular distribution of histamine in mouse brain neurons. Inflamm. Res. 51 (Suppl. 1), S46–S48.
Mikkelsen, J.D., Panula, P., Moller, M., 1992. Histamine-immunoreactive nerve fibers in the rat pineal gland: evidence for a histaminergic central innervation. Brain Res. 597, 200–208.
Miklos, I.H., Kovacs, K.J., 2003. Functional heterogeneity of the responses of histaminergic neuron subpopulations to various stress challenges. Eur. J. Neurosci. 18, 3069–3079.
Molina-Hernandez, A., Diaz, N.F., Arias-Montano, J.A., 2012. Histamine in brain development. J. Neurochem. 122, 872–882.
Motta, S.C., Guimaraes, C.C., Furigo, I.C., Sukikara, M.H., Baldo, M.V., Lonstein, J.S., Canteras, N.S., 2013. Ventral premammillary nucleus as a critical sensory relay to the maternal aggression network. Proc. Natl. Acad. Sci. U. S. A. 110, 14438–14443.
Nagaishi, V.S., Cardinali, L.I., Zampieri, T.T., Furigo, I.C., Metzger, M., Donato Jr., J., 2014. Possible crosstalk between leptin and prolactin during pregnancy. Neuroscience 259, 71–83.
Nakamura, K., Morrison, S.F., 2011. Central efferent pathways for cold-defensive and febrile shivering. J. Physiol. 589, 3641–3658.
Nakamura, W., Yamazaki, S., Nakamura, T.J., Shirakawa, T., Block, G.D., Takumi, T., 2008. In vivo monitoring of circadian timing in freely moving mice. Curr. Biol. 18, 381–385.
Nissinen, M.J., Karlstedt, K., Castren, E., Panula, P., 1995. Expression of histidine decarboxylase and cellular histamine-like immunoreactivity in rat embryogenesis. J. Histochem. Cytochem. 43, 1241–1252.
Nissinen, M.J., Panula, P., 1995. Developmental patterns of histamine-like immunoreactivity in the mouse. J. Histochem. Cytochem. 43, 211–227.
Panula, P., Happola, O., Airaksinen, M.S., Auvinen, S., Virkamaki, A., 1988. Carbodiimide as a tissue fixative in histamine immunohistochemistry and its application in developmental neurobiology. J. Histochem. Cytochem. 36, 259–269.
Panula, P., Sundvik, M., Karlstedt, K., 2014. Developmental roles of brain histamine. Trends Neurosci. 37, 159–168.
Parmentier, R., Ohtsu, H., Djebbara-Hannas, Z., Valatx, J.L., Watanabe, T., Lin, J.S., 2002. Anatomical, physiological, and pharmacological characteristics of histidine decarboxylase knock-out mice: evidence for the role of brain histamine in behavioral and sleep-wake control. J. Neurosci. 22, 7695–7711.
Paxinos, G., Watson, C., 2005. The Rat Brain in Stereotaxic Coordinates, 5th ed. Elsevier Academic Press, MA, USA.
Phillips, A.J., Fulcher, B.D., Robinson, P.A., Klerman, E.B., 2013. Mammalian rest/activity patterns explained by physiologically based modeling. PLoS Comput. Biol. 9, e1003213.
Pollard, H., Pachot, I., Schwartz, J.C., 1985. Monoclonal antibody against L-histidine decarboxylase for localization of histaminergic cells. Neurosci. Lett. 54, 53–58.

Provensi, G., Coccurello, R., Umehara, H., Munari, L., Giacovazzo, G., Galeotti, N., Nosi, D., Gaetani, S., Romano, A., Moles, A., Blandina, P., Passani, M.B., 2014. Satiety factor oleoylethanolamide recruits the brain histaminergic system to inhibit food intake. Proc. Natl. Acad. Sci. U. S. A. 111, 11527–11532.

Puelles, L., Martinez-de-la-Torre, M., Bardet, S., Rubenstein, J., 2012. Hypothalamic nuclei derived from the diverse progenitor domains. In: Watson, C., Paxinos, G., Puelles, L. (Eds.), The Mouse Nervous System. Academic Press, London, UK, pp. 255–295.

Rezai-Zadeh, K., Yu, S., Jiang, Y., Laque, A., Schwartzenburg, C., Morrison, C.D., Derbenev, A.V., Zsombok, A., Munzberg, H., 2014. Leptin receptor neurons in the dorsomedial hypothalamus are key regulators of energy expenditure and body weight, but not food intake. Mol. Metab. 3, 681–693.

Rozov, S.V., Zant, J.C., Karlstedt, K., Porkka-Heiskanen, T., Panula, P., 2014. Periodic properties of the histaminergic system of the mouse brain. Eur. J. Neurosci. 39, 218–228.

Sakata, T., Yoshimatsu, H., Masaki, T., Tsuda, K., 2003. Anti-obesity actions of mastication driven by histamine neurons in rats. Exp. Biol. Med. (Maywood) 228, 1106–1110.

Saper, C.B., Lu, J., Chou, T.C., Gooley, J., 2005. The hypothalamic integrator for circadian rhythms. Trends Neurosci. 28, 152–157.

Sasaki, M., Radtke, C., Tan, A.M., Zhao, P., Hamada, H., Houkin, K., Honmou, O., Kocsis, J.D., 2009. BDNF-hypersecreting human mesenchymal stem cells promote functional recovery, axonal sprouting, and protection of corticospinal neurons after spinal cord injury. J. Neurosci. 29, 14932–14941.

Schwartz, M.D., Nunez, A.A., Smale, L., 2009. Rhythmic cFos expression in the ventral subparaventricular zone influences general activity rhythms in the Nile grass rat, *Arvicanthis niloticus*. Chronobiol. Int. 26, 1290–1306.

Smolen, A.J., Wright, L.L., Cunningham, T.J., 1983. Neuron numbers in the superior cervical sympathetic ganglion of the rat: a critical comparison of methods for cell counting. J. Neurocytol. 12, 739–750.

Staines, W.A., Daddona, P.E., Nagy, J.I., 1987. The organization and hypothalamic projections of the tuberomammillary nucleus in the rat: an immunohistochemical study of adenosine deaminase-positive neurons and fibers. Neuroscience 23, 571–596.

Sunkin, S.M., Ng, L., Lau, C., Dolbeare, T., Gilbert, T.L., Thompson, C.L., Hawrylycz, M., Dang, C., 2013. Allen Brain Atlas: an integrated spatio-temporal portal for exploring the central nervous system. Nucleic Acids Res. 41, D996–D1008.

Takatsu, Y., Matsumoto, H., Ohtaki, T., Kumano, S., Kitada, C., Onda, H., Nishimura, O., Fujino, M., 2001. Distribution of galanin-like peptide in the rat brain. Endocrinology 142, 1626–1634.

Torrealba, F., Yanagisawa, M., Saper, C.B., 2003. Colocalization of orexin a and glutamate immunoreactivity in axon terminals in the tuberomammillary nucleus in rats. Neuroscience 119, 1033–1044.

Turenius, C.I., Charles, J.R., Tsai, D.H., Ebersole, P.L., Htut, M.H., Ngo, P.T., Lara, R.N., Stanley, B.G., 2009. The tuberal lateral hypothalamus is a major target for GABAA – but not GABAB-mediated control of food intake. Brain Res. 1283, 65–72.

Umehara, H., Mizuguchi, H., Fukui, H., 2012. Identification of a histaminergic circuit in the caudal hypothalamus: an evidence for functional heterogeneity of histaminergic neurons. Neurochem. Int. 61, 942–947.

Umehara, H., Mizuguchi, H., Mizukawa, N., Matsumoto, M., Takeda, N., Senba, E., Fukui, H., 2010. Innervation of histamine neurons in the caudal part of the arcuate nucleus of hypothalamus and their activation in response to food deprivation under scheduled feeding. Methods Find. Exp. Clin. Pharmacol. 32, 733–736.

Umehara, H., Mizuguchi, H., Mizukawa, N., Matsumoto, M., Takeda, N., Senba, E., Fukui, H., 2011. Deprivation of anticipated food under scheduled feeding induces c-Fos expression in the caudal part of the arcuate nucleus of hypothalamus through histamine H(1) receptors in rats: potential involvement of E3 subgroup of histaminergic neurons in tuberomammillary nucleus. Brain Res. 1387, 61–70.

Vanhala, A., Yamatodani, A., Panula, P., 1994. Distribution of histamine-, 5-hydroxytryptamine-, and tyrosine hydroxylase-immunoreactive neurons and nerve fibers in developing rat brain. J. Comp. Neurol. 347, 101–114.

Wada, H., Inagaki, N., Itowi, N., Yamatodani, A., 1991. Histaminergic neuron system: morphological features and possible functions. Agents Actions Suppl. 33, 11–27.

Wagner, U., Segura-Torres, P., Weiler, T., Huston, J.P., 1993. The tuberomammillary nucleus region as a reinforcement inhibiting substrate: facilitation of ipsihypothalamic self-stimulation by unilateral ibotenic acid lesions. Brain Res. 613, 269–274.

Watanabe, T., Taguchi, Y., Shiosaka, S., Tanaka, J., Kubota, H., Terano, Y., Tohyama, M., Wada, H., 1984. Distribution of the histaminergic neuron system in the central nervous system of rats; a fluorescent immunohistochemical analysis with histidine decarboxylase as a marker. Brain Res. 295, 13–25.

Yoshida, K., McCormack, S., Espana, R.A., Crocker, A., Scammell, T.E., 2006. Afferents to the orexin neurons of the rat brain. J. Comp. Neurol. 494, 845–861.

Yoshimatsu, H., Chiba, S., Tajima, D., Akehi, Y., Sakata, T., 2002. Histidine suppresses food intake through its conversion into neuronal histamine. Exp. Biol. Med. (Maywood) 227, 63–68.

Yu, X., Zecharia, A., Zhang, Z., Yang, Q., Yustos, R., Jager, P., Vyssotski, A.L., Maywood, E.S., Chesham, J.E., Ma, Y., Brickley, S.G., Hastings, M.H., Franks, N.P., Wisden, W., 2014. Circadian factor BMAL1 in histaminergic neurons regulates sleep architecture. Curr. Biol. 24, 2838–2844.

Zhao, P., Shao, Y.F., Zhang, M., Fan, K., Kong, X.P., Wang, R., Hou, Y.P., 2012. Neuropeptide S promotes wakefulness through activation of the posterior hypothalamic histaminergic and orexinergic neurons. Neuroscience 207, 218–226.